

An experimental study of Wiffle ball aerodynamics

Jenn Rossmann^{a)} and Andrew Rau

Department of Mechanical Engineering, Lafayette College, Easton, Pennsylvania 18042

(Received 21 December 2006; accepted 28 August 2007)

We measure the aerodynamic forces on a Wiffle ball as a function of the Reynolds number and ball orientation. The effects of asymmetric flow outside the ball and flow within the ball are considered, and are both associated with the ball's tendency to curve without pitcher-imparted spin. The problem of Wiffle ball aerodynamics is an accessible way to introduce topics such as boundary layer separation and transition to turbulence. © 2007 American Association of Physics Teachers.
[DOI: 10.1119/1.2787013]

I. INTRODUCTION

The game of Wiffle ball is a variant of baseball played with a plastic perforated ball. Eight 3/4 in. oblong holes affect half the surface area of the Wiffle ball, while the other hemisphere is uninterrupted. According to the Wiffle ball company's publicity materials, the ball was invented via trial and error by David Mullany in 1952.¹ The ball was originally designed to rest the arm of a young pitcher (Mullany's son) and achieves a curving trajectory without requiring the pitcher to impart spin or hurl at top speed. Figure 1 shows the Wiffle company's illustrated pitching instructions.

Although the aerodynamics of baseball have been of significant interest for over half a century,²⁻⁶ the physics of a Wiffle ball's performance have not been much investigated. That the ball attains a curved trajectory solely due to the positioning of the holes, with little need for spin, can be confirmed in play, but researchers have not formally examined the flow patterns, forces, and physics involved.

The pattern of holes on the Wiffle ball, like the stitching on a baseball or seam on a cricket ball, can create an asymmetric flow field. Whether the ball tends to curve toward or away from those holes is a matter of some contention.⁷⁻⁹ Two experts debated the question in *The Atlantic Monthly*.¹⁰ Robert Adair speculated that the holes, like the stitching on a baseball, accelerate a transition to turbulence on the perforated side of the Wiffle ball. The faster flow over the perforated side might lower the pressure and cause the ball to move toward the holes. Peter Brancazio countered that scuffing a Wiffle ball "essentially takes the holes out of the equation:" if the smooth, unperforated side of the ball were sufficiently roughened, it might disturb the air more than the holes, reversing the pressure asymmetry and causing the ball to curve away from the holes.¹⁰ Others, such as the inventor of a competing perforated practice ball, argue that the curve of the Wiffle ball is simply random.¹¹

The Wiffle ball was not considered in Mehta's thorough survey of the aerodynamics of sports balls,¹² although many of the issues involved might be similar to those in the flight of baseballs and cricket balls. The asymmetric flow field caused by the Wiffle ball holes could yield the same result as does the Magnus effect on a spinning baseball: a trajectory that curves or bends in the direction of the resulting pressure force. However, rather than simply flowing over the ball surface, air may also flow through a Wiffle ball, which distinguishes a Wiffle ball from other sports balls. Although Wiffle aficionados acknowledge its effects,⁹ it is not clear how significant this airflow is to the aerodynamics.

An investigation of the aerodynamics of Wiffle balls might provide new physical understanding of flow phenomena and

additional insight into baseball aerodynamics. In the following we discuss wind tunnel experiments and analytical studies and clarify the major issues associated with the aerodynamics of Wiffle balls. The relevant fluid mechanical forces are quantified, and the effect of the ball orientation is examined.

II. EXPERIMENTAL METHOD

Experiments were performed in a subsonic 12 in. × 12 in. open-circuit wind tunnel. The forces normal and parallel to the direction of airflow were measured with a strain gauge-based force sting balance manufactured by Aerolab¹³ and with a student-designed instrument capable of measuring forces on a spinning ball.^{14,15}

The ball was mounted in the test section of the wind tunnel, and its orientation is characterized by the angle α between the oncoming airflow and the horizontal (the conventional angle of attack), the angle θ between the horizontal and the axis of the perforation formation, and the angle β between the oncoming airflow and the axis of the perforation formation, or $\alpha + \theta$. This geometry is illustrated in Fig. 2. An angle of attack of $\alpha = 0^\circ$, and the holes positioned facing the oncoming airflow, corresponds to angle $\beta = 0^\circ$; $\beta = 90^\circ$ corresponds to a ball at zero angle of attack with the holes on top, as in the center image of Fig. 1.

Dimensionless numbers are of much value in fluid dynamics. One of the most important dimensionless numbers is the Reynolds number, the ratio of the fluid inertia to its viscosity. The Reynolds number is defined as

$$\text{Re} = \frac{\rho V d}{\mu}, \quad (1)$$

where ρ is the fluid (air) density, V is the fluid free-stream velocity, d is the diameter of the Wiffle ball, and μ is the fluid (air) viscosity. A Wiffle ball is 7.2 cm in diameter and weighs 20 g. Wind speeds of 10–100 mph were tested, corresponding to Reynolds numbers ranging from 2×10^4 to 2×10^5 . Typical Wiffle ball pitches are expected to be concentrated in the low end of this regime.

Wind speeds were measured with a Pitot-static probe, and point measurements of velocity were also made using a Dwyer PFH hot-wire anemometer.¹⁶ The anemometer had a 0.2 s response time, making it well suited for instantaneous velocity measurements. Both sting balances had diameters of approximately $0.1d$ and lengths of approximately $2.5d$. Images and measurements were taken with side, bottom, and



Fig. 1. Instructions for throwing a Wiffle ball (Ref. 1).

rear-mounted balances, with the sting placement having minimal influence on both flow patterns observed and forces measured.

The measured normal forces, F_N and axial F_A , were converted to lift F_L and drag F_D forces using the angle of attack α in Eq. (2).

$$F_L = F_N \cos \alpha - F_A \sin \alpha$$

$$F_D = F_A \cos \alpha + F_N \sin \alpha. \quad (2)$$

The lift and drag are characterized by their dimensionless coefficients:

$$C_{L,D} = \frac{F_{L,D}}{(1/2)\rho V^2 A}, \quad (3)$$

where A is the frontal area of the Wiffle ball. For a sphere, the drag coefficient C_D is expected to decrease until $Re = 10^3$, and then to remain reasonably constant in the range $10^3 < Re < 10^5$.¹⁷ This constant value is around 0.5 for smooth spheres.¹⁷ The drag drop or drag crisis, the abrupt decrease in drag with the transition to turbulent flow, occurs in the range $1 \times 10^5 < Re < 3 \times 10^5$ for smooth spheres and at lower Re for rough spheres. Previous studies have found that the lift coefficient on a spinning sphere is strongly correlated with the spin number ($Sn = \pi d \omega / V$, the ratio of ball rotation speed to bulk air speed) and, to a lesser extent, with Re .^{3,4}

III. RESULTS

A. Drag

The drag coefficient C_D was found to decrease from a maximum near 1 at the lowest airspeeds tested to a value of approximately 0.4–0.6 at higher Reynolds numbers, depending on the ball orientation. These trends are shown in Fig. 3. Drag data for a nonspinning baseball¹⁸ are also included for comparison. Good agreement is observed between the base-

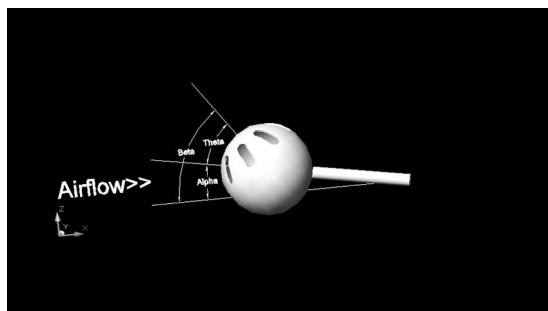


Fig. 2. Orientation of Wiffle ball for wind tunnel experiments.

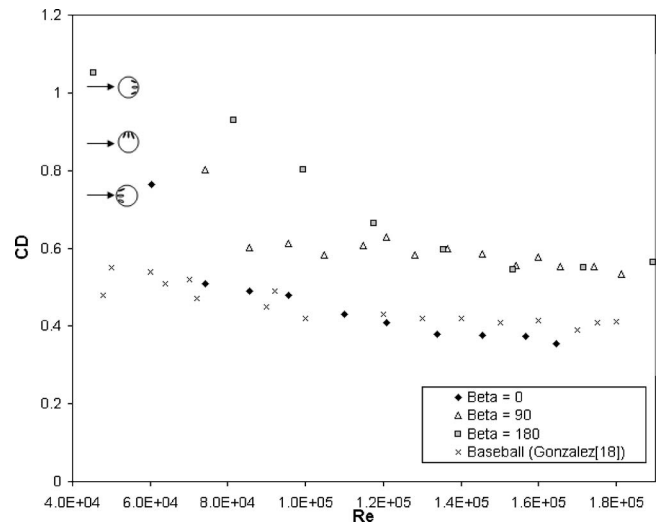


Fig. 3. Wiffle ball drag coefficient as function of the Reynolds number for various orientations.

ball and the Wiffle ball oriented at $\beta=0$, for which the perforations (much like baseball stitching) may induce turbulent flow in the boundary layer.

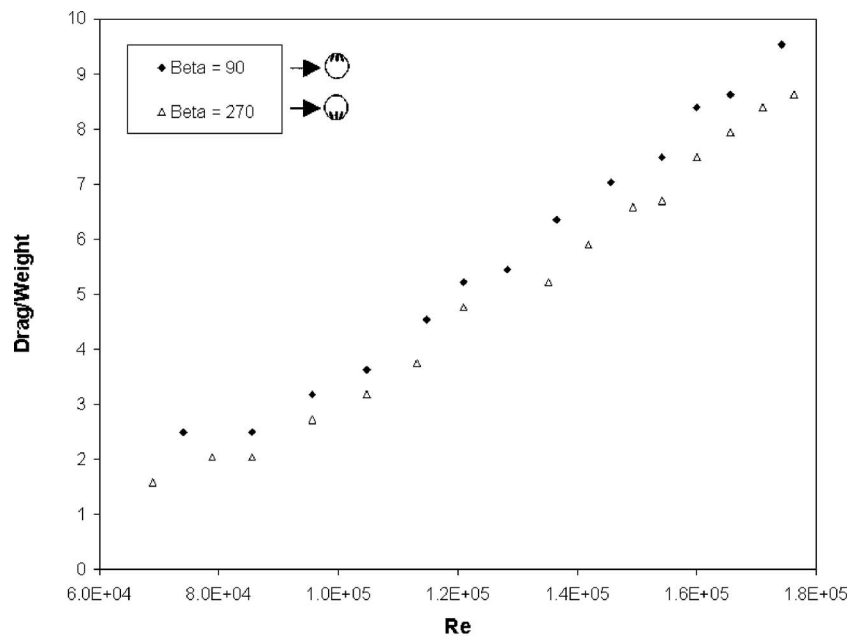
The consideration of the ratio of drag to ball weight highlights the impact of the Wiffle ball's low weight on its trajectory. The ratio of drag to Wiffle ball weight as a function of Reynolds number for two values of β is shown in Fig. 4(a). The same relation was observed when the holes are on the side of the ball; little dependence on ball orientation was observed. These curves follow the accepted trend for a nonspinning baseball,⁴ as demonstrated by Fig. 4(b). The trends are also similar to data on smooth spheres.¹⁷

B. Lift

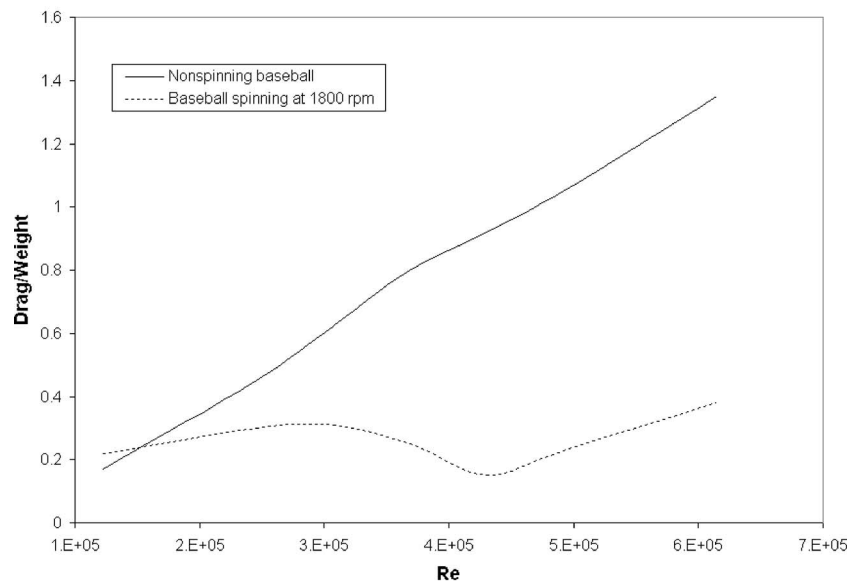
The Wiffle ball was found to have lift forces that are strongly dependent on ball orientation. For air speeds above 30 mph and small values of β (positive or negative), the direction of the lift force was away from the Wiffle perforation formation: an upward lift force was observed if the ball's holes were in the southern hemisphere, and a downward or negative lift force if the holes were in the northern hemisphere. The deflection of the wake corresponding to a negative lift can be clearly seen using a fog tracer as shown in Fig. 5.

The magnitude of the measured lift force also depends on the ball orientation. The influence of the angle β on the lift force measured at a fixed speed ($Re = 1 \times 10^5$) can be seen in Fig. 6. For $|\beta| \leq 45^\circ$ the lift force was directed opposite to the hole position: holes positioned at a negative angle corresponded to an upward force on the ball; a positive angle resulted in a downward force. The transition between these two regimes, $\beta=0^\circ$, corresponds to a Wiffle ball orientation often said to produce a random knuckleball.^{1,8} We imagine that small perturbations of the ball would cause dramatic changes in its trajectory if the lift force changed sign in flight.

For the same range of ball orientations, the effect of Reynolds number was also investigated. When the holes faced the oncoming airflow, holes in the near northern hemisphere ($0^\circ < \beta \leq 45^\circ$) resulted in a negative lift that increased in magnitude with increasing velocity, and holes in the near



(a)



(b)

Fig. 4. (a) Drag-to-weight ratio for a Wiffle ball as function of Re . (b) Drag-to-weight ratio for a baseball as function of Re (see Ref. 4).

southern hemisphere ($315^\circ \leq \beta < 360^\circ$, or $-45^\circ \leq \beta < 0^\circ$) resulted in positive lift that also increased in magnitude with increasing velocity. These trends are shown in terms of the lift-to-weight ratio in Fig. 7. Although the lift forces themselves are not especially large, they have a significant effect on the Wiffle ball's flight.

For holes positioned at larger angles from the oncoming flow, the lift forces measured were directed toward the holes. Values of the lift coefficient for the ball orientation in the middle of Fig. 1, with $\beta=90^\circ$, are shown in Fig. 8. The measured lift force increases in magnitude with increasing velocity. The maximum values of the lift coefficient that were measured, 0.35–0.4, would be achieved by a baseball at a spin number of approximately 0.5.³

Because the typical release speeds for pitched Wiffle balls are in the lower range of our measurements, trends at lower

air speeds (up to 45 mph) are of particular interest. The aerodynamics in this range lends credence to the anecdotal experience of random and unstable ball behavior. For example, the dataset for $\beta=345^\circ$ also includes a change of sign in the lift from negative to positive at a Reynolds number of approximately 5.5×10^4 , as shown in Fig. 9. This change of sign was observed for some but not all orientations, and was not observed in the potentially symmetric case of $\beta=15^\circ$, which highlights the need for further studies in the lower speed regime.

When the holes are on the downstream side of the Wiffle ball, the trends are less clear cut. For values of β between 90° and 270° , the correlation between the lift force and hole orientation was much weaker than when the holes faced the oncoming air. This finding is not surprising due to the presence of separated wake flow on the downstream side.

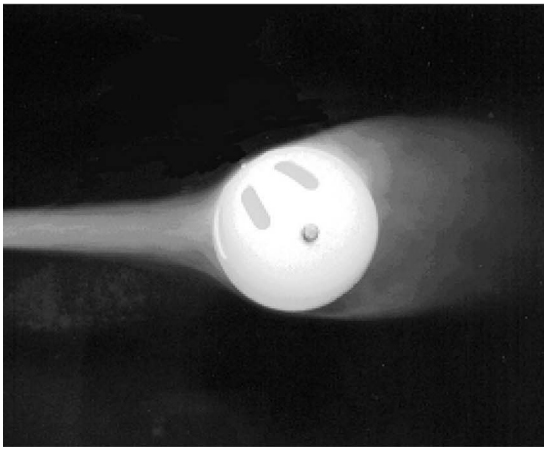
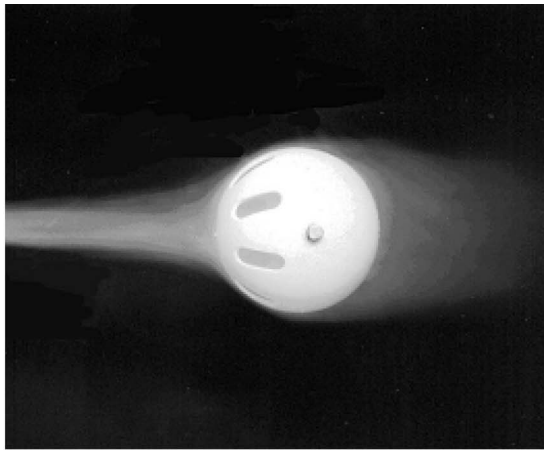


Fig. 5. (a) Symmetric layout of Wiffle ball holes. (b) Upward deflection of Wiffle ball wake due to asymmetric position of the holes. Fog visualization images taken at $Re=4 \times 10^4$. The observations were determined to be independent of string balance position.

C. Lateral force

Another important factor in predicting the trajectory of a pitched ball is the side or lateral force on the ball.^{3,5} The side force was measured on a ball with the holes positioned to one side at an azimuthal angle of $\pm 90^\circ$. (This angle, like β , reflects the angle between oncoming airflow and the axis of the perforation formation; however, in this case the perforations are on the side of the ball.) A lateral force in the direction toward the holes, increasing in magnitude with increasing air speed, was measured. This side force is shown as a function of Reynolds number in Fig. 10. The ratio of the lateral force to Wiffle ball weight is used to emphasize the significant effect that even a small lateral force can have on the Wiffle trajectory. These observations are consistent with those of the Wiffle ball manufacturer, who indicate (cf. the left and right images in Fig. 1) their expectation of a lateral force directed toward the holes positioned on the side of the pitched Wiffle ball.

D. Flow within ball

A hot wire anemometer was used to measure the wind speed inside the ball. The ball was oriented with the holes in the northern hemisphere, symmetric about the vertical axis, so that $\beta=90^\circ$. These measurements showed that there was significant axial air flow inside the ball. Figure 11 shows the wind speed measured at $0.4d$ inside the ball relative to the wind speed outside the ball. At this location, the internal air speed is generally about 25% of the magnitude of the free-stream flow. Figure 11 clearly illustrates that the wind speed inside the ball increases with the wind speed outside the ball. The influence of the position on flow conditions inside the ball is demonstrated by Fig. 12. The anemometer measurements reflected a turbulence level (velocity fluctuations relative to the mean free-stream flow) of approximately 7–8% within the Wiffle ball, which may be compared with a free-stream turbulence level of 1% or less in the wind tunnel. However, the apparent turbulence of the velocity measured may have been due to reversing flow or some unsteady flow phenomena.

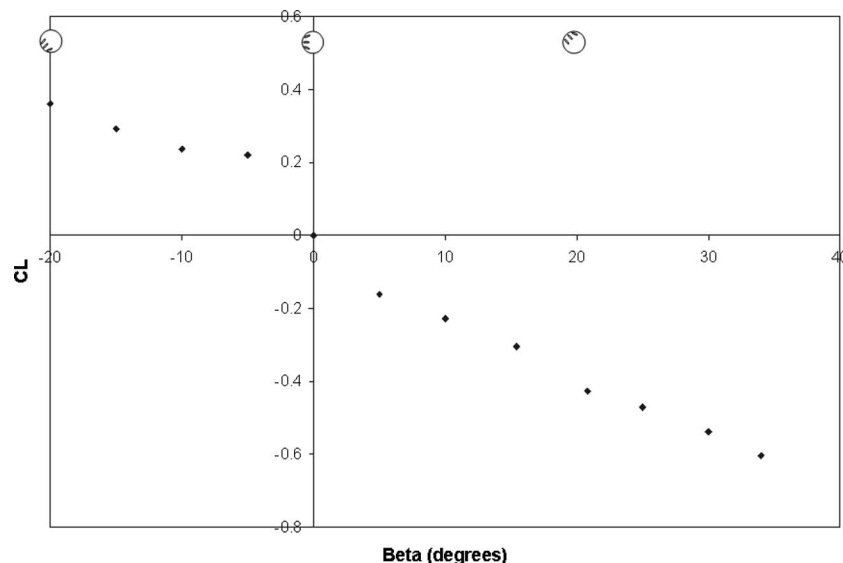


Fig. 6. Variation of lift coefficient with ball orientation characterized by the angle β at $Re=1 \times 10^5$.

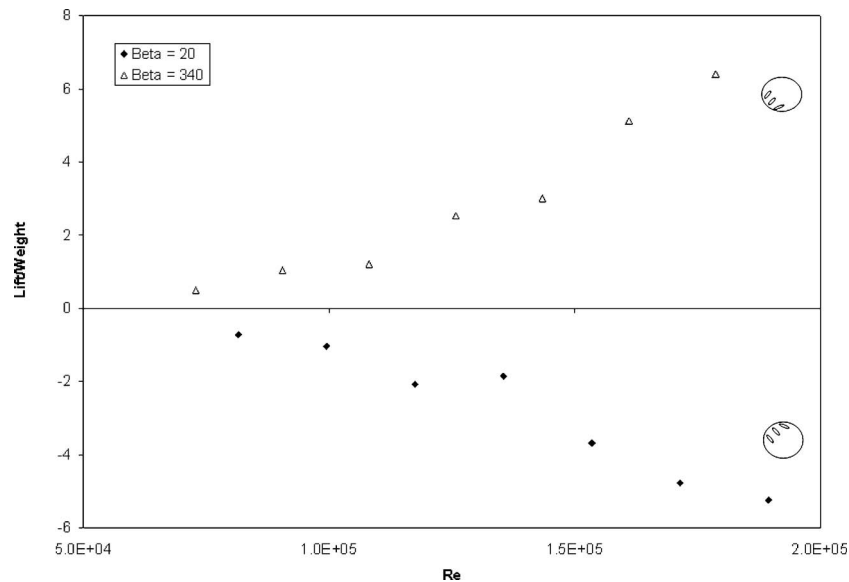


Fig. 7. Lift-to-weight ratio for a Wiffle ball as function of Re for holes oriented in the northern ($\beta > 0^\circ$) and southern ($\beta < 0^\circ$) hemispheres.

IV. MEASUREMENT UNCERTAINTY

Wind tunnel measurements are complicated by the low weight of the Wiffle ball. The lift, drag, and lateral forces are small, requiring signal amplification and the use of lift-to-weight and drag-to-weight ratios to determine the influence of even small forces on Wiffle ball flight dynamics. Our experimental protocol included recalibration of the flow speed instrumentation using a Pitot-static probe and differential manometer before each trial to ensure that the velocity measurements used in calculations were accurate to within 5% and repeatable. An analysis of the measurement uncertainty gives lift and drag values accurate to within 10% and generally to within 5%.

V. DISCUSSION

The drag coefficient found for the ball at higher Reynolds numbers ($Re \geq 1.4 \times 10^5$) was approximately 0.4 to 0.6, depending on ball orientation. The drag coefficient for a smooth sphere in the same Reynolds number range is 0.5. It is reasonable to expect the Wiffle ball holes to initiate turbulence in the boundary layer, causing a drag drop to occur at lower Reynolds number than for a smooth ball. Based on the drag data obtained, this early transition to turbulence does not appear to have occurred for all ball orientations.

The idea that the Wiffle ball holes induce a transition to turbulence would also suggest that boundary layer separation would be delayed on the hemisphere of the ball affected by

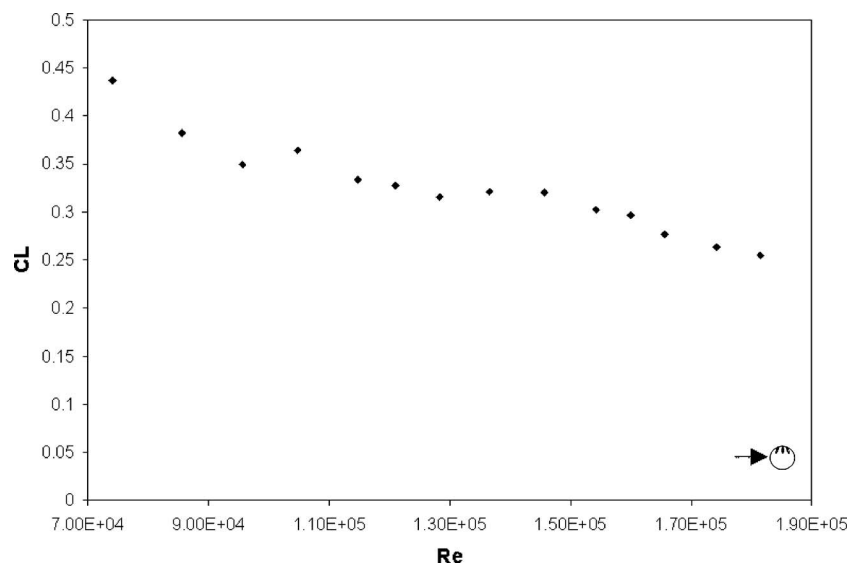


Fig. 8. The lift coefficient as a function of the Reynolds number for a ball with $\beta = 90^\circ$.

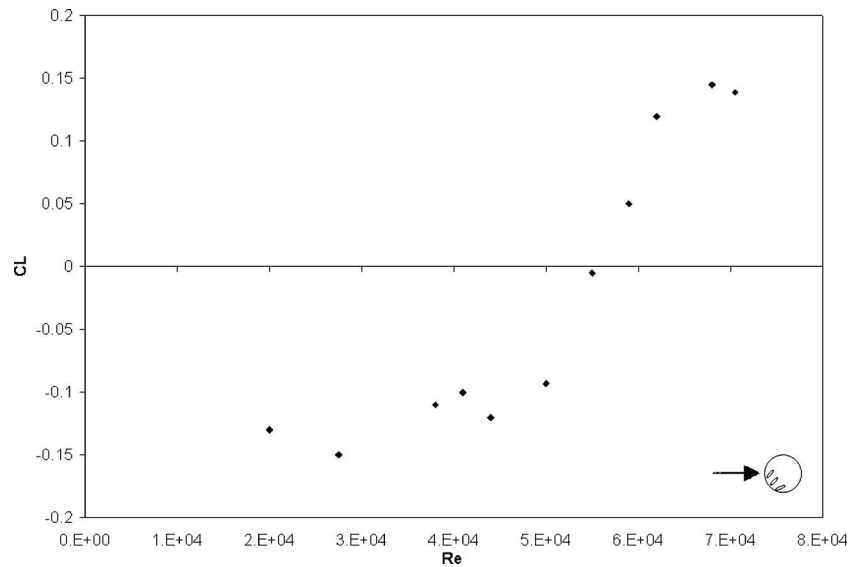


Fig. 9. The change of sign of the lift coefficient versus Reynolds number for $\beta=345^\circ$.

the holes, resulting in a force in the same direction as the holes. However, this force orientation was not observed in our study. Nor were forces found to be random, as suspected by Wiffle ball competitors and batters who've just struck out. For values of $|\beta| \leq 45^\circ$, and particularly when the Wiffle ball holes were on the upstream side of the ball, a force was measured that opposed the position of the holes. For larger values of β , the lift force was consistently directed toward the holes. Holes positioned 90° from the oncoming flow in any direction resulted in a (lift or lateral) force directed toward the holes. These behaviors were confirmed by flow visualization.

The fact that the correlation of the lift with the position was stronger when the holes were on the upstream portion of the ball implies that some airflow is captured within the ball, and that a captured downward airflow or downwash effect induces a force on the ball. The generation of forces, and in

particular the enhancement of lift by trapped vortices, has been demonstrated in wing aerodynamics¹⁹ and combustion²⁰ applications. The larger drag coefficient may also be the result of a trapped vortex flow inside the Wiffle ball and the interruption of the wake.

The airflow inside the Wiffle ball was measured to be somewhat more turbulent than that outside the ball, and to reach velocities 25% of the free-stream values. Perhaps this internal flow plays a role in determining the ball's trajectory. An internal vortex or internal "downwash" flow pattern is consistent with the measured forces.

It is most likely that two aerodynamic forces—one due to the disruption of exterior boundary layer flow by the holes, and one due to the flow inside the ball—compete over whether the force on a Wiffle ball is in the same or opposite direction to the holes. The asymmetric boundary layer separation appears to be dominant at lower velocities ($Re < 3$

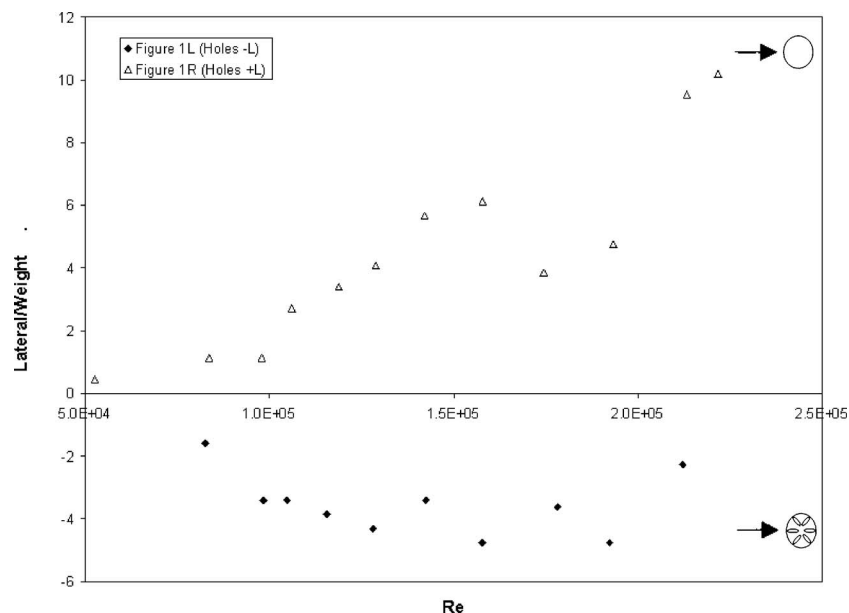


Fig. 10. The ratio of lateral force to Wiffle ball weight as a function of Re for holes on the side of ball. Positive lateral force is into the page in ball schematics.

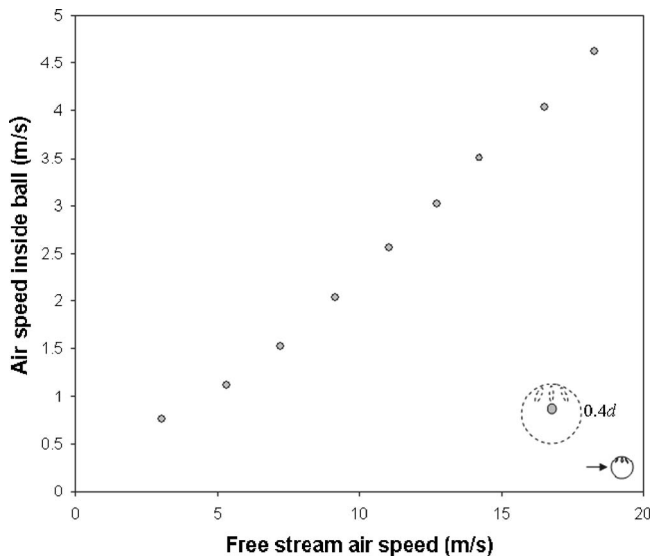


Fig. 11. Velocity $0.4d$ inside the Wiffle ball versus the free stream (outside) velocity. $\beta=90^\circ$.

$\times 10^4$), while the internal flow results in a flow that can be directed opposite the holes for $Re > 4 \times 10^4$. In the range of airspeeds between these thresholds, nuances such as ball scuffing may be decisive.

VI. CONCLUSIONS

The aerodynamic forces on a Wiffle ball depend on ball orientation and speed. The force along the axis of Wiffle ball perforations is directed away from the Wiffle perforations for small values of β , and toward the Wiffle holes for larger angles. There is a measurable airflow inside the Wiffle ball, with velocities equal to approximately 25% of the free-stream velocity outside the ball. The effect of this internal air flow may be in competition with external aerodynamics (asymmetric boundary layer separation due to the Wiffle holes) for control of the ball's trajectory.

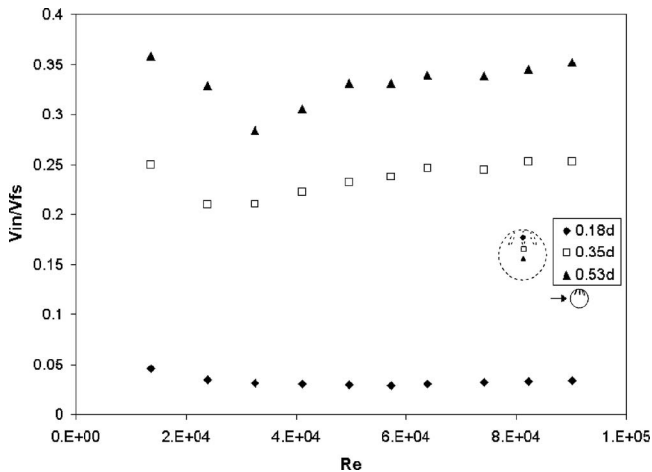


Fig. 12. The ratio of the velocity inside the Wiffle ball to the free stream velocity, V_{in}/V_{fs} , at three positions inside the Wiffle ball. $\beta=90^\circ$.

Further studies of the Wiffle ball should include analytical and numerical modeling as well as experiments. Potential flow models created in the current study have yielded results in good agreement with the experimental data. To gain a more detailed understanding of the boundary layer flow, high-resolution measurements of flow velocity would be valuable. Although Wiffle balls are thrown with much less pitcher-imparted spin than are baseballs, it may be interesting to include the effects of this spin in future studies.

The flow inside the Wiffle ball is of great interest and appears to be the cause of an effective spin on the ball. Careful examination of this internal flow is necessary to determine whether it is a trapped vortex flow as seems likely. Experiments performed in close cooperation with computations will further illuminate the aerodynamics of Wiffle balls. Such studies have the potential to introduce complex fluid mechanical phenomena to students in an accessible context.

ACKNOWLEDGMENTS

The authors gratefully acknowledge the support of the Lafayette College EXCEL Scholars program, Harvey Mudd College, and the National Science Foundation. They are also in the debt of Sheldon Logan, Alexis Utvich, Toby Rossmann, and Colin Jemmott.

^aElectronic address: rossmanj@lafayette.edu

¹Documentation enclosed with Wiffle® Ball, The Wiffle® Ball, Shelton, CT 02003.

²L. Briggs, "Effect of spin and speed on the lateral deflection (curve) of a baseball and the Magnus effect for smooth spheres," *Am. J. Phys.* **27**, 589–596 (1959).

³R. G. Watts and R. Ferrer, "The lateral force on a spinning sphere: Aerodynamics of a curveball," *Am. J. Phys.* **55**(1), 40–44 (1987).

⁴R. Adair, *The Physics of Baseball* (Harper Collins, New York, 2002).

⁵R. G. Watts and T. A. Bahill, *Keep Your Eye on the Ball: Curve Balls, Knuckleballs and Fallacies of Baseball* (W. H. Freeman, New York, 2000).

⁶M. K. McBeath, "The rising fastball—baseball's impossible pitch," *Perception* **19**(4), 545–552 (1990).

⁷C. Bergquist, "Super-fly ball," *Science World* **60**(14), 4–5 (2004).

⁸M. Palinczar, spokesman, New Jersey Wiffle Ball Association, Trenton, NJ.

⁹K. Kochev, "The physics of Wiffleball—Parts I and II," *FastPlastic 12 and 13*, (www.fastplastic.net) (2004).

¹⁰L. Green, "The Wiffle effect," *The Atlantic Monthly* **289**(6), 88 (2002).

¹¹D. McGinn, "A whole new ball game," *Wired* **11**(11), 38 (2003).

¹²R. D. Mehta, "Aerodynamics of sports balls," *Annu. Rev. Fluid Mech.* **17**, 151–189 (1985).

¹³Aerolab, Laurel, MD 20723

¹⁴Y. H. Hsu, C. M. Stratton, J. M. Schauer, A. Utvich, and J. S. Rossmann, "Design and construction of a new subsonic wind tunnel," *ASME International Mechanical Engineering Congress Proceedings*, MECE2003-4M853, Washington, D.C., 2003, pp. 710–715.

¹⁵C. W. Jemmott and J. S. Rossmann, "Aerodynamics of spinning spheres—A new correlation" (unpublished).

¹⁶Dwyer Instruments, Michigan City, IN 46361.

¹⁷B. R. Munson, D. F. Young, and T. H. Okiiski, *Fundamentals of Fluid Mechanics* (Wiley, Hoboken, NJ, 2006).

¹⁸Richard Gonzalez, "Aerodynamics of a knuckleball," Honors thesis in mechanical engineering, Tulane University, 1968.

¹⁹V. J. Rossow, "Lift enhancement by an externally trapped vortex," *J. Aircr.* **15**(9), 618–625 (1978).

²⁰V. R. Katta and W. M. Roquemore, "Study on trapped-vortex combustor—effect of injection on flow dynamics," *J. Propul. Power* **14**(3), 273–281 (1998).